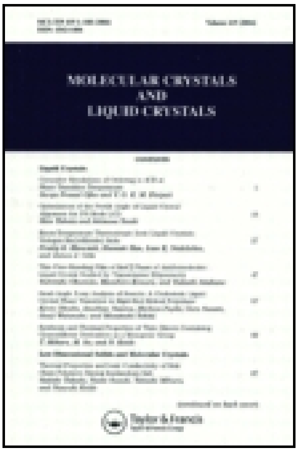

Molecular Crystals and Liquid Crystals
Publication details, including instructions for authors and subscription information:
http://www.tandfonline.com/loi/gmcl20

# $Mg_xC_{60}$ Fabricated by Using $Mg:C_{60}$ Co-Evaporation Method for Carrier Doping

N. Ohashi [a], T. Miyadera [a], T. Taima [a] [b] & Y. Yoshida [a]

[a] The Research Center for Photovoltaics, National Institute of Advanced Industrial Science and Technology (AIST), Central, Higashi, Tsukuba, Ibaraki, Japan

[b] JST-PRESTO, Japan Science and Technology Agency (JST), Honcho Kawaguchi, Saitama, Japan

To cite this article: N. Ohashi, T. Miyadera, T. Taima & Y. Yoshida (2011): $Mg_xC_{60}$ Fabricated by Using $Mg:C_{60}$ Co-Evaporation Method for Carrier Doping, Molecular Crystals and Liquid Crystals, 538:1, 193-198

To link to this article: http://dx.doi.org/10.1080/15421406.2011.563723

*Mol. Cryst. Liq. Cryst.*, Vol. 538: pp. 193–198, 2011

ISSN: 1542-1406 print/1563-5287 online
DOI: 10.1080/15421406.2011.563723

Taylor & Francis
Taylor & Francis Group

# $Mg_xC_{60}$ Fabricated by Using $Mg:C_{60}$ Co-Evaporation Method for Carrier Doping

N. OHASHI,[1] T. MIYADERA,[1] T. TAIMA,[1,2] AND
Y. YOSHIDA[1]

[1]The Research Center for Photovoltaics, National Institute of Advanced Industrial Science and Technology (AIST), Central, Higashi, Tsukuba, Ibaraki, Japan
[2]JST-PRESTO, Japan Science and Technology Agency (JST), Honcho Kawaguchi, Saitama, Japan

*$Mg{:}C_{60}$ co-evaporation method has been performed to obtain fulleride of $Mg_xC_{60}$ thin films for carrier doping. Atomic concentration of the film has been examined by x-ray photoelectron spectroscopy to calibrate the composition ratio, and the results indicated that Mg concentration in the film was controlled well. Then, crystal structure of the $Mg{:}C_{60}$ mixing film has been examined by using grazing incidence x-ray diffraction method. The diffraction patterns suggested that these films were microcrystalline $Mg_xC_{60}$. Conductivity of the mixing films was increased as composition ratio of Mg increasing. It indicates that Mg atoms acted as carrier dopant.*

**Keywords** Co-evaporation; grazing incidence X-ray diffraction (GIXD); $Mg_xC_{60}$; X-ray photoelectron spectroscopy (XPS)

## Introduction

Contact resistance within electrode/semiconductor interface is becoming a critical limiting factor in conventional organic photovoltaics, because series resistance degrades short-circuit current and fill factor. For that reason, the contact resistance must be decreased for further improvement of the efficiency. It is known that carrier doping in the vicinity of the interface decreases the contact resistance. Because high carrier doping decreases thickness of depletion layer, and it results in enhancing tunnel injection [1]. It is known that alkali and alkaline-earth metals doping for fullerene ($C_{60}$) exhibit high conductivity and metallic behavior [2–4]. As an exception, Mg-doped $C_{60}$ keeps semiconductor property [5,6], which means we are able to modulate the conductivity and Fermi level of Mg-doped $C_{60}$. It is suggested that Mg-doped $C_{60}$ have a high potential as n-type organic semiconductor. Chikamatsu and co-workers reported that photovoltaics using top Mg:Ag electrode instead of Al electrode reduced the contact resistance [7]. It is indicated that Mg atoms diffused or

---

Address correspondence to N. Ohashi, The Research Center for Photovoltaics, National Institute of Advanced Industrial Science and Technology (AIST), Central 5, 1-1-1, Higashi, Tsukuba, Ibaraki 305-8565, Japan. Tel.: +81-29-861-6397; Fax: +81-29-861-6232; E-mail: noboru-oohashi@aist.go.jp

implanted into $C_{60}$ layer, and in that case, Mg atoms acted as carrier dopant. However, these types of doping technique have serious problem as follows. Diffusion or implantation method is difficult to control dopant density and distribution. It is especially disadvantage particularly for the thin film devices. Moreover, ion implantation in $C_{60}$ leads to disintegration of $C_{60}$ molecules [8]. By contrast, co-evaporation method is suitable for thin film devices, because we can control dopant density and distribution. Mg doped $C_{60}$ film by using co-evaporation method is worth to study more.

In this study, we fabricated $C_{60}$:Mg co-evaporated film, then, examined structural and electrical characteristics of the film. We confirmed that fulleride of $Mg_xC_{60}$ was also obtained by the co-evaporation method.

## Experimental Details

Polished Si (100) substrate was used as substrate. Substrate was cleaned with ultra sonication and UV/$O_3$ treatment. Mg:$C_{60}$ mixing film was fabricated by co-evaporation in high-vacuum chamber ($10^{-6}$ Pa). Deposition rate of $C_{60}$ was controlled at 1 nm/min, and deposition rate of Mg was changed to control the composition ratio. Deposition rate was measured by quartz crystal deposition controller (*ULVAC* CRTM-6000). Since sticking probability is varied with surface conditions composition ratio was calibrated with atomic concentration examined by X-ray photoelectron spectroscopy (XPS). XPS measurements were performed by Quantum 2000 (*ULVAC-PHI*) in *AIST Nano-Processing Facility*. Crystal structure of the thin films was then examined by grazing incidence x-ray diffraction (GIXD). GIXD measurement was performed by ATX-G (*RIGAKU*) at beamline BL46XU of *SPring-8*. Conductivity of Mg:$C_{60}$ mixing films was examined by four-point probe (FPP) method (*KYOWARIKEN* K-705RS).

## Results and Discussions

Atomic concentration of the Mg:$C_{60}$ mixing film was examined by XPS to calibrate the composition ratio. In most case, atomic concentration of the top surface is different from that of the bulk because of the surface contaminant. We cleaned the surface of samples by Ar sputtering to avoid this issue. XPS depth profile of Mg:$C_{60}$ mixing film was shown in Figure 1. Atomic concentration of the top surface was different from that of bulk, which indicating surface contamination of the film. We therefore used the value of bulk to reduce experimental error. We note that organic materials are usually degraded by Ar sputtering. Some researcher used $C_{60}$ ion beam and succeeded to minimize the sample degradation [9]. In the case of low degradation samples, XPS spectrum shows no change in intensity throughout the sputtering process. Here, the XPS depth profiles shown in Figure 1 were almost constant value at the bulk region. Therefore, sputtering degradation of our work was negligible. Composition ratio was transformed into the ratio of deposition rate using following equation;

$$\frac{DR_{\mathrm{Mg}}D_{\mathrm{Mg}}}{DR_{\mathrm{C60}}D_{\mathrm{C60}}} = \frac{n_{\mathrm{Mg}}}{n_{\mathrm{C60}}} \cdot \frac{M_{\mathrm{Mg}}}{M_{\mathrm{C60}}}, \tag{1}$$

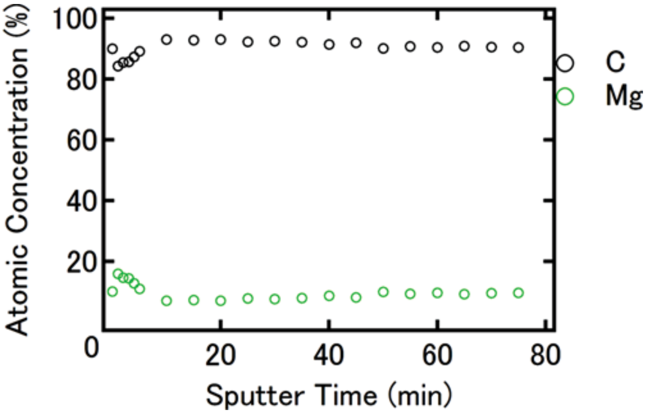

**Figure 1.** The XPS depth profile of Mg:$C_{60}$ mixing film. Argon ion was used for sputtering. Sputter voltage was 1000 V. Sputter time of 0 min indicates top surface of the Mg:$C_{60}$ film.

where, $DR_{Mg}$ is deposition rate of Mg [m/s], $DR_{C60}$ is deposition rate of $C_{60}$ [m/s], $D_{Mg}$ is density of Mg [kg/m], $D_{Mg}$ is density of $C_{60}$ [kg/m] $n_{Mg}$ is amount of substance of Mg [mol], $n_{C60}$ is amount of substance of $C_{60}$ [mol], $M_{Mg}$ is atomic weight of Mg, $M_{C60}$ is molecular weight of $C_{60}$, respectively. Then, composition ratio obtained from deposition rate of quartz crystal deposition controller was calibrated by that of XPS. Figure 2 shows result of the calibration. Calibrated composition ratio was proportional to the square root of the deposition rate. It indicates that Mg concentration in the mixing film was controlled well. For the application of electric devices, it is necessary to control not only doping density but also dopant distribution. Since it was probable that Mg atoms diffused into $C_{60}$ layer, Mg density distribution was examined by XPS depth profile. Figure 3 shows XPS depth profile of Mg:$C_{60}$/$C_{60}$ stacking film. Three different layers were identified in Figure 3.

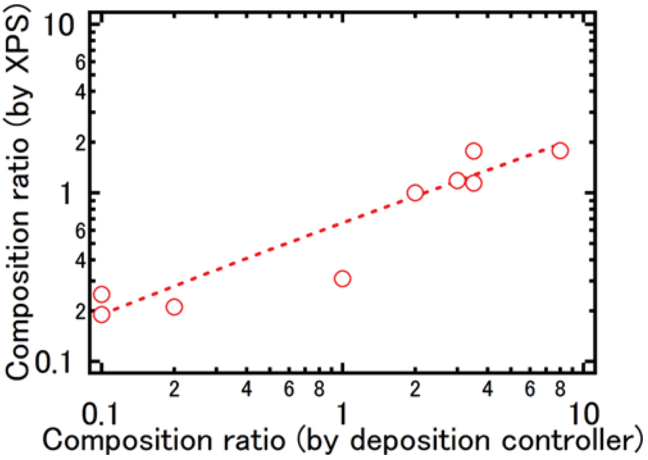

**Figure 2.** Calibrated result of composition ratio by atomic concentration ratio obtained by XPS. Dashed line indicates fitted curve.

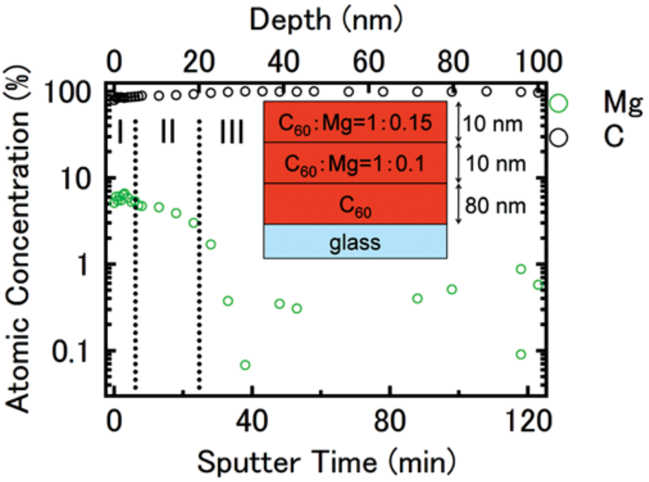

**Figure 3.** The XPS depth profile of Mg:$C_{60}$ mixing film. Inset shows the sample dimensions. Three layers with different composition ratio were stacked.

Boundary positions between each layer were not clear, because spatial resolution of the XPS depth profile in this study was about 10 nm. Mg atoms were still observed at pure $C_{60}$ layer (3rd layer) in the range of 0.1–1%. It indicates noise level because there was no Mg peak in the XPS spectra. On the basis of above discussions, noticeable diffusion of Mg atoms into $C_{60}$ layer was not occurred by performing co-evaporation.

Crystal structure of Mg:$C_{60}$ mixing films was then examined by x-ray diffraction method. Since co-evaporated film was very thin (about 100 nm), GIXD method was used in this work. It is known that mixture of alkaline-earth atom and $C_{60}$ produces fullerides of $A_xC_{60}$. The alkaline-earth atoms occupy the octahedral and the tetrahedral interstitial site of $C_{60}$ lattice [6]. Doping of Mg atoms results in the crystalline phase transition from face-centered cubic to rhombohedral. It is reported that $Mg_4C_{60}$ is indexed with lattice parameters $a = b = 9.22$ Å, $c = 25.25$ Å, $\gamma = 120°$ [10]. It is also reported that $Mg_xC_{60}$ ($x = 1.3$–$6.5$) keeps rhombohedral phase [11]. Here, Figure 4 shows summary of the x-ray diffraction pattern of Mg:$C_{60}$ co-evaporated films. Each Mg:$C_{60}$ profiles show broad peak at intermediate position between (022) and (113) of pristine $C_{60}$. These peaks were indexed as (110) of $Mg_xC_{60}$, which is only appeared in rhombohedral phase of $Mg_xC_{60}$. Therefore, Mg:$C_{60}$ films fabricated by co-evaporation have a rhombohedral phase of $Mg_xC_{60}$. Weak and broad peaks in Mg:$C_{60}$ mixing films suggested that disordered microcrystal was grown on the substrate. In particular, diffraction peaks of Mg:$C_{60}$ = 1.8:1 film were almost disappeared. It indicates that high doping of Mg prevent crystal forming; result in a practical limitation of dopant density. Although poor crystallinity produces carrier mobility degradation, improving crystallinity of the co-evaporated film is necessary for the application of electric devices such as organic photovoltaics. Substrate temperature and deposition rate are taking a key role to improve mobility of organic thin films [12]. Several researchers reported that the mobility and crystallinity of vacuum evaporated $C_{60}$ films were improved as substrate temperature increasing [13–15]. In addition, Itaka and co-workers reported that crystallinity of $C_{60}$ on flat pentacene monolayer were much improved [16].

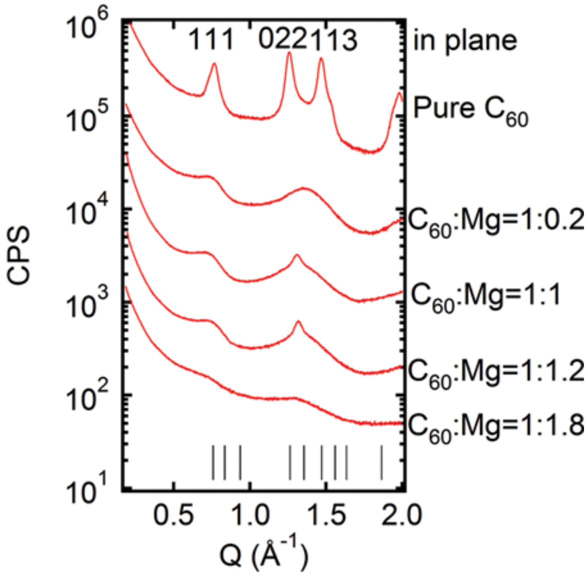

**Figure 4.** Summary of the x-ray diffraction pattern of the Mg:$C_{60}$ mixing films. Ticks indicate reflection positions of $Mg_xC_{60}$. Grazing angle and wavelength of x-ray was 0.14° and 1.1807 Å, respectively.

We expect that the mobility and crystallinity of $Mg_xC_{60}$ was improved by the same manner.

Then, conductivity of Mg:$C_{60}$ mixing films was measured by four-point-probe method. Figure 5 shows conductivity vs. composition ratio plot. Conductivity of the film abruptly increased at Mg:$C_{60}$ = 1:1, then, conductivity increased as composition ratio of Mg increasing. Mg atomic density in the film is in this condition was about $10^{22}\,\mathrm{cm}^{-3}$. In other words, enhancement of conductivity was only shown in quite high dopant density. It indicates that Mg:$C_{60}$ mixing films in this work contain

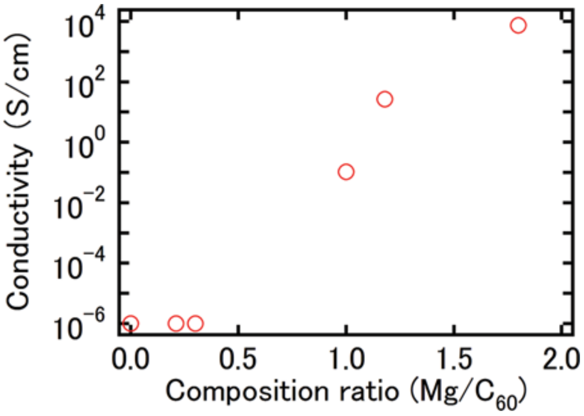

**Figure 5.** Conductivity vs. composition ratio plot obtained by FPP method. Electrode pitch and diameter of the probe was 1 mm and 150 $\mu$m, respectively.

high carrier trap density and very low mobility because of poor crystallinity of the film which was suggested in Figure 4.

## Conclusion

In conclusion, we have fabricated Mg:$C_{60}$ mixing films by using co-evaporation method. Atomic concentration of the film was examined by XPS, and we found that Mg concentration in the film was controlled well. GIXD and FPP measurement confirmed that we have succeeded to make the fulleride of $Mg_xC_{60}$, and Mg acted as carrier dopant. Further improvement of the crystallinity will be necessary for the application of electric devices such as organic photovoltaics.

## Acknowledgment

This work was partly supported by *New Energy and Industrial Technology Development Organization* (NEDO) of Japan.

## References

[1] Sze, S. M. (1981). *Physics of Semiconductor Devices*, 2nd ed. Wiley: New York, US.

[2] Haddon, R. C., Hebard, A. F., Rosseinsky, M. J., Murphy, D. W., Duclos, S. J., Lyons, K. B., Miller, B., Rosamilia, J. M., Fleming, R. M., Kortan, A. R., Glarum, S. H., Makhija, A. V., Muller, A. J., Eick, R. H., Zahurak, S. M., Tycko, R., Dabbagh, G., & Thiel, F. A. (1991). *Nature*, *350*, 320.

[3] Haddon, R. C., Kochanski, G. P., Hebard, A. F., Fiory, A. T., & Morris, R. C. (1992). *Science*, *258*, 1636.

[4] Chikamatsu, M., Kazaoui, S., Minami, N., Yase, K., Kodama, T., Nishikawa, H., Ikemoto, I., & Kikuchi, K. (2002). *Mol. Cryst. Liq. Cryst.*, *377*, 353.

[5] Chen, Y., Stepniak, F., Weaver, J. H., Chibante, L. P. F., & Smalley, R. E. (1992). *Phys. Rev. B*, *45*, 8845.

[6] Gupta, R. P., & Gupta, M. (1994). *Physica. C.*, *219*, 21.

[7] Chikamatsu, M., Taima, T., Yoshida, Y., Saito, K., & Yase, K. (2004). *Appl. Phys. Lett.*, *84*, 127.

[8] Narayanan, K. L., Yamaguchi, M. (2003). *Sol. Energy Mater. & Sol. Cells*, *75*, 345.

[9] Sanada, N., Yamamoto, A., Oiwa, R., & Ohashi, Y. (2004). *Surf. Interface Anal*, *36*, 280.

[10] Boronidics, F., Oszlányi, G., Faigel, G., & Pekker, S. (2003). *Solid State Commun.*, *127*, 311.

[11] Heguri, S. Ph.D. thesis. *University of Hyogo (2009).* (in Japanese).

[12] Nakamura, M., Ohguri, H., Goto, N., Tomii, H., Xu, M. S., Miyamoto, T., Matsubara, R., Ohashi, N., Sakai, M., & Kudo, K. (2009). *Appl. Phys. A*, *95*, 73.

[13] Anthopoulos, T. D., Singh, B., Marjanovic, N., Sariciftci, N. S., Ramil, A. M., Sitter, H., Cölle, M., & de Leeuw, D. M. (2006). *Appl. Phys. Lett.*, *89*, 212504.

[14] Ohashi, H., Tanigaki, K., Kumashiro, R., Sugihara, S., Hiroshiba, S., Kimura, S., Kato, K., & Takata, M. (2004). *Appl. Phys. Lett.*, *84*, 520.

[15] Singh, Th. B., Sariciftci, N. S., Yang, H., Yang, L., Plochberger, B., & Sitter, H. (2007). *Appl. Phys. Lett.*, *90*, 213512.

[16] Itaka, K., Yamashiro, M., Yamaguchi, J., Haemori, M., Yaginuma, S., Matsumoto, Y., Kondo, M., & Koinuma, H. (2006). *Adv. Mater.*, *18*, 1713.